

---

# Performance analysis of burst-mode receivers with clock phase alignment and forward error correction for GPON

Bhavin J. Shastri Julien Faucher Noha Kheder  
Ming Zeng Nicholas Zicha David V. Plant

Received: 15 December 2007 / Revised: 20 August 2008 / Accepted: 20 August 2008 / Published online: 11 October 2008  
Springer Science+Business Media, LLC 2008

**Abstract** We experimentally demonstrate the performance analysis of burst-mode receivers (BMRx) in a 622 Mb/s 20-km gigabit-capable passive optical network (GPON) uplink. Our receiver features automatic phase acquisition using a clock phase aligner (CPA), and forward-error correction using (255, 239) Reed-Solomon (RS) codes. The BMRx provides instantaneous (0 preamble bit) phase acquisition and a packet-loss ratio (PLR)  $\leq 10^{-6}$  for any phase step ( $\leq 2\pi$  rads) between consecutive packets,

(P2MP); using time division multiple access (TDMA), multiple ONUs transmit bursty data in the 1310-nm window to the OLT in the central office (CO). To use the shared medium effectively, the ONUs require a burst-mode transmitter with a short turn-on/off delay [7]. Because of optical path differences in the upstream path, packets can vary in phase and amplitude. To deal with these variations, the OLT requires a burst-mode receiver (BMRx). The BMRx is responsible for amplitude and phase recovery, which must be achieved at the beginning of every packet. At the front-end of the BMRx is a burst-mode limiting amplifier (BM-LA) responsible for amplitude recovery. Then, clock-and-data recovery (CDR) is performed with phase acquisition by a clock phase aligner (CPA). The most

a longer physical reach or support more splits per single PON tree. Our BMRx meets the GPON PMD layer specifications as specified in the G.984.2 standard [9].

We also study the impact of MPN in the uplink in terms of the effective BER and PLR coding gain. We investigate the PLR performance of the system and quantify it as a function of the phase step between consecutive packets, received signal power, consecutive identical digits (CIDs) immunity, and BER. We also assess the tradeoffs in preamble length, power penalty, and pattern correlator error resistance. In addition, we demonstrate how the CPA and the RS(255, 239) codes can be used in conjunction to account for dynamic burst-error correction giving reliable BERs in bursty channels. These results will help refine theoretical models of BMRx and PONs, and provide input for establishing realistic power budgets.

The rest of the paper is organized as follows. In Sect. 2, we present the GPON experimental setup. The design and implementation of the BMRx is described in Sect. 3. Section 4 is devoted to the presentation and analysis of the experimental results. Finally, the paper is summarized and concluded in Sect. 5.

## 2 GPON experimental setup

A block diagram of the GPON uplink experimental setup is shown in Fig. 2. A 1310-nm laser is modulated with upstream PON traffic using an electro-optic modulator (EOM). The modulated signal is then sent through 20 km of uplink single-mode fiber (SMF-28). The desired information rate is 622 Mb/s. As the RS(255, 239) code introduces  $\approx 15/14$  overhead, we use an aggregate bit rate of 666.43 Mb/s. A variable optical attenuator (VOA) serves to control the received power level. The optical to electrical conversion is performed by a photodetector. The electrical signal is then low-pass filtered (LPF) by a fourth-order Bessel-Thomson filter whose 3-dB cutoff frequency is  $0.7 \times$  bit rate, or 467 MHz. Such a filter has an optimum bandwidth to filter out noise while keeping inter-symbol interference (ISI) to a minimum [14].

A typical bursty signal that complies with PON standards is used as a test signal in our experiments and is depicted in Fig. 3. Packet 1 serves as a dummy packet to force the burst-mode CDR to lock to a certain phase  $\phi_1$  before the arrival of packet 2 with phase  $\phi_2$ . The BER and PLR measurements are performed on packet 2 only. Packet 2 consists of 16 guard bits, 0–28 (l) preamble bits, 20 delimiter bits,  $2^{15} - 1$  payload bits, and 48 comma bits. The guard, preamble, and delimiter bits correspond to the physical-layer upstream burst-mode overhead of 8 bytes at 622 Mb/s as specified by the G.984.2 standard [9]. The guard bits provide distance between two consecutive packets to avoid collisions. The preamble is split into two fields, a threshold determination field (TDF) for amplitude recovery and a CPA field for clock-phase recovery. The delimiter is a unique pattern indicating the start of the packet to perform byte synchronization. Likewise, the comma is a unique pattern to indicate the end of the payload. The payload is simply a non-return-to-zero (NRZ)  $2^{15} - 1$  pseudorandom binary sequence (PRBS). The PLR and the BER are measured on the payload bits only. We define the lock acquisition time corresponding to the number of bits (l) needed in front of the delimiter in order to get error-free operation, that is, a zero PLR for over 3 min of operation at 622 Mb/s ( $[10^6$  packets received, i.e.,  $\text{PLR} \setminus 10^{-6}$ ), a  $\text{BER} \setminus 10^{-10}$ , and for any phase step ( $\Delta\phi$ )

$$T_{s_1} = m \frac{u}{2p} T$$

where  $T$

1

the payload of the packets. The BERT compares the incoming data with an internally generated  $2^{15} - 1$  PRBS. Note that, while a conventional BERT can be used to make the BER measurements, PLR measurements on discontinuous, bursty data, is not supported. This is because conventional BERTs require a continuous alignment between the incoming pattern and the reference pattern, and milliseconds to acquire synchronization. The phase step response of the burst-mode CDR can make conventional BERTs lose pattern synchronization at the beginning of every packet while the sampling clock is being recovered by the CDR. The custom BERT does not require fixed synchronization between the incoming pattern and the reference pattern of the error detector. Synchronization happens instantaneously at the beginning of every packet, therefore enabling PLR measurements on discontinuous, bursty data.

#### 4 Experimental results and discussions

In this section, we experimentally study the effect of channel impairments on the performance of BMRx in the GPON uplink. The BMRx performance is quantified in terms of the BER and PLR measurements. More specifically, the following measurements are taken: BER versus signal power, PLR versus phase step, signal power, CID immunity, and BER. We also assess various tradeoffs and penalties in the preamble length, power budget, and pattern correlator error resistance. In addition, we investigate the impact of MPN in the uplink in terms of the effective PLR and BER coding gain. Where appropriate, comparisons between theoretical predictions and experimental results hav-7.6Pf-7.687.8-456.6(and)-4in

$$t = \frac{n - k}{2} \quad (4)$$

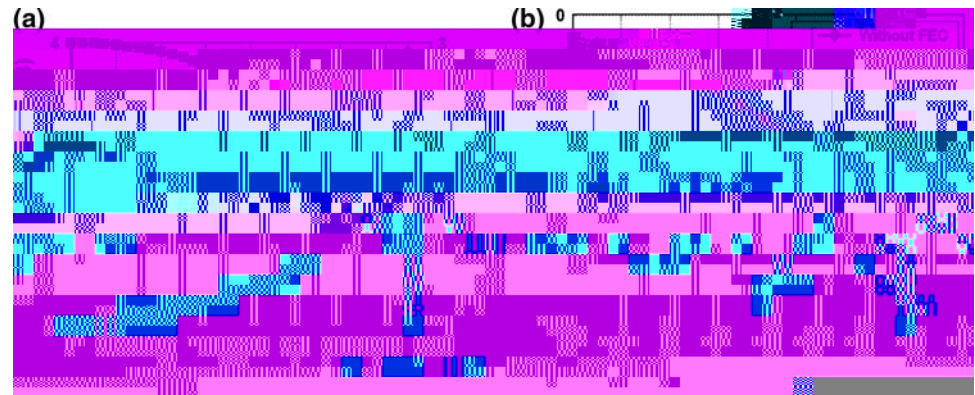
and  $t$  is the symbol error correcting capability of the code. Note that  $\lfloor x \rfloor$  represents the largest integer not to exceed  $x$ . Again, assuming a memoryless channel and since we are using orthogonal signaling (ON-OFF keying), the lower bound of the BER after FEC  $p_e^{\text{FEC}}$ , can be calculated as

$$p_e^{\text{FEC}} \geq \frac{p_s^{\text{FEC}}}{m} \quad (5)$$

We plot the purely random and memoryless channel prediction of the BER after FEC  $p_e^{\text{FEC}}$ , and our experimental results in Fig. 5. The BER performance is a function of intrinsic<sup>1</sup> and extrinsic<sup>2</sup> effects of the channel [16]. Thus, the presence of random and deterministic errors will affect the error correcting capability of the FEC code. It can be observed that the experimental and the theoretical results are in close agreement for BER  $[10^{-4}]$ . This is because for lower signal power, random errors dominate over deterministic errors in the system. However



Fig. 7 (a) Effective coding gain and MPN penalty after FEC versus mean square variance of MPN. (b) Theoretical determination of effective coding gain with the worst-case MPN assuming only random errors in GPON uplink



phase of the incoming packet. To understand how the CPA works, consider the case when there is no phase step ( $\Delta\phi = 0$  rad); path O correctly samples the incoming pattern (see  $t_{\text{odd}}$  in Fig. 8(g)). For phase step  $\Delta\phi = \pi/2$  (400 ps) rads, path E will sample the bits on or close to the transitions after the phase step (see  $t_{\text{even}}$  in Fig. 8(h)). In this situation, the byte synchronizer of path E will likely not detect the delimiter at the beginning of the packet. On the other hand, the byte synchronizer of path O will have no problems detecting the delimiter (see  $t_{\text{odd}}$  in Fig. 8(h)). The phase picker controller monitors the state of the two byte synchronizers and selects the correct path accordingly (path O in this particular case). Once the selection is made, it cannot be overwritten until the comma is detected, indicating the end of the packet. This process repeats itself at the beginning of every packet. The result is that the CPA achieves instantaneous phase acquisition (0-bit) for any phase step ( $\Delta\phi = 2\pi$  rads), that is, no preamble bits at the beginning of the packet are necessary. We further discuss these results in the next section.

#### 4.4 Packet-loss ratio versus phase step

In this section, we investigate the PLR performance of the GPON uplink as a function of the phase step between consecutive packets. Let us first consider the case for a back-to-back configuration (without the 20-km of uplink fiber). Figure 9(a) shows PLR versus phase step performance, with only the CDR and the CPA turned off. We have restricted the horizontal axis to values from  $0 \leq \Delta\phi \leq 1600$  ps, corresponding to  $0 \leq \Delta\phi \leq 2\pi$  phase difference at the desired bit rate ( $\approx 622$  Mb/s). Also, note that the results are symmetrical about 0 rad from  $2\pi \leq \Delta\phi \leq 0$  rads. We observe a bell-shaped curve centered at 800 ps because this represents the half bit period corresponding to the worst-case phase step at  $\Delta\phi = \pi$  rads, and therefore, the CDR is sampling exactly at the edge of the data eye. Jitter would have led to the worst case phase ( $\pi$  rad) being displaced from 800 ps. Hence, we conclude that jitter is not significant in our measurements. At relatively small phase shifts (near 0 or

Fig. 8 (a–c) Bursty traffic (packets with different phases) input signal to the receiver with phase steps:  $\Delta\phi = 0$  rad (0 ps),  $\Delta\phi = \pi/2$  rads (400 ps), and  $\Delta\phi = \pi$  rads (800 ps). (d–f) Response of the CDR to bursty traffic. (g–i) Response of the  $2\times$  oversampling CDR to bursty traffic and the depiction of the odd and even samples resulting from  $t_{\text{odd}}$  and  $t_{\text{even}}$  sampling instants





2p rad), we can easily achieve zero PLR with the CPA module disabled because the CDR is almost sampling at the middle of each bit (refer to Fig. 8(a)).

Preamble bits ("1010

with, the PLR performance of the CDR is then comparable to the PLR performance obtained by the BMRx which does not require any preamble bits. Hence, there is a tradeoff between the power penalty with the BMRx oversampling when  $\mu = 0$  rad and the number of preamble bits required without the BMRx when  $\mu \neq 0$ .



Fig. 13 PLR versus signal power for different MPN mean square variances in GPON uplink

resistance to  $z = 2$  bits, we obtain improvement in the PLR performance by eight orders of magnitude.

In Sect. 4.2, we studied the effect of MPN on the uplink in terms of the BER performance of the system. It is also interesting to see the effect that MPN has on the PLR performance of the system. In Fig. 13, we plot the PLR for various values of the mean square variance of MPN  $r_{mpn}$ . As expected, the system performance degrades with an increase in  $r_{mpn}$ . Recall that the maximum MPN that can be tolerated in the uplink giving an effective coding gain of zero, is when  $r_{mpn} = 0.14$ . At this value of MPN, there is a deterioration of more than two orders of magnitude in the PLR for signal power = 13 dBm. However, by increasing the pattern correlator error resistance to  $z = 2$  bits, we observe a coding gain of  $\approx 2$  dB at a PLR =  $10^{-6}$  which can be used to compensate for the MPN penalty and also the 1-dB burst-mode penalty (see Fig. 10(a)).

#### 4.8 Dynamic burst-error correction

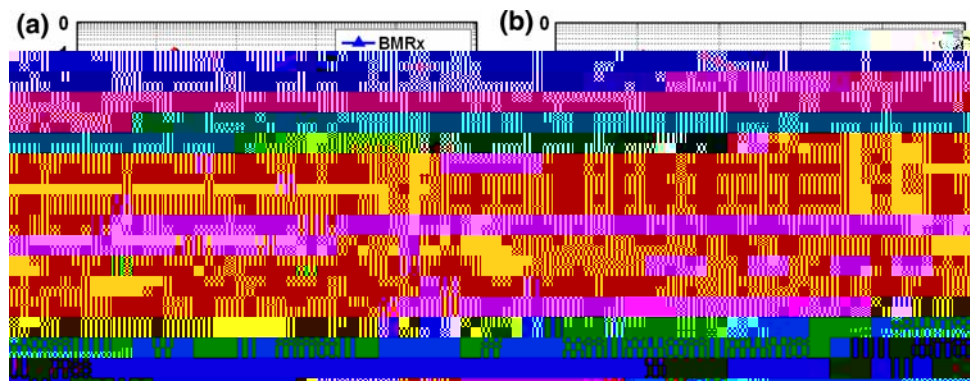
A burst-error is defined as an  $n$ -bit sequence that contains clustered bit errors. Two erroneous bits always mark the

first and last bits of the sequence, and there can be any number of errors, up to  $(n - 2)$ , in between them [21]. Burst-errors inherently arise in GPON uplink because of the phase acquisition process by CDRs for bursty data. This makes the BER measurements unreliable and unpredictable, and therefore not a true representation of BER. There are two comments on this. First, at a particular signal power, the BER may not converge because of the presence of burst-errors from packet to packet. Thus, the BER can change from measurement to measurement for the same signal power. Second, the BER will also vary for packets with different phases at the same signal power. This is because the phase acquisition time of the CDR is a function of the relative phase difference between two packets.

RS codes can be useful for burst-error correction provided that the burst length is less than the codes' error correcting capability 0. However, there is no such guarantee in a GPON uplink because the signal power and the phase difference between packets vary in burst-mode reception from packet to packet. Burst-error correcting codes have been demonstrated for bursty channels [22–26], but these codes introduce complexity at the circuit level implementation. On the other hand, RS codes are relatively simple. Our technique of employing FEC with RS codes in a BMRx with fast phase acquisition provides a simple solution to correct for burst-errors in a GPON uplink.

In Fig. 14, the BER and the PLR performance of the system is monitored as function of packet reception. Let us first consider the case with the CPA and FEC turned off (see Fig. 14(a)), and the signal power is such that the BER =  $10^{-4}$ . Starting with no phase difference between the consecutive packets,  $\phi = 0$  rad and switching the FEC on, the RS(255, 239) codes help obtain a BER =  $10^{-10}$  as expected. However, with a phase step,  $\phi = 0$  rad introduced in the uplink, the following can happen: first, the phase difference can result in a poor PLR with almost all the packets being lost as shown in Fig. 14(b). Note that BER measurements can only be made on packets that are received. This means that with almost all packets lost, the BER obtained will be unreliable. A packet lost may be

Fig. 14 BER and PLR performance versus number of received packets in GPON uplink



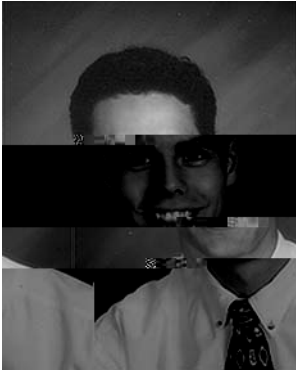
retransmitted. However, despite any number of retransmissions, there is no guarantee that the packets will be received

through the Alexander Graham Bell Canada Graduate Scholarship (CGS), McGill University through the Lorne Trottier Engineering Fellowship and McGill Engineering Doctoral Award (MEDA), Le Fonds Québécois de la Recherche sur la Nature et les Technologies (FQRNT) through graduate scholarships, by industrial and government partners through the Bell Canada NSERC Industrial Research Chair (IRC), the NSERC-funded Agile All-Photonic Networks (AAPN) Research Network, and by the Canadian Institute for Photonic Innovation (CIPI).

## References

1. Girard, A. (2005). FTTx PON technology and testing. Quebec City, QC, Canada: Electro-Optical Engineering Inc., 1-55342-006-3.
2. Lee, C.-H., Sorin, W. V., & Kim, B. Y. (2006). Fiber to the home using a PON infrastructure. *IEEE Journal of Lightwave Technology*, 24(12), 4568–4583.
3. Abrams, M., Becker, P. C., Fujimoto, Y., O’Byrne, V., & Piehler, D. (2005). FTTP deployments in the United States and Japan—equipment choices and service provider imperatives. *IEEE Journal of Lightwave Technology*, 23(1), 236–246.
4. Wagner, R. E., Igel, J. R., Whitman, R., Vaughn, M. D., Ruffin, A. B., & Bickham, S. (2006). Fiber based broadband-access deployment in the United States. *IEEE Journal of Lightwave Technology*, 24(12), 4526–4540.
5. Koonen, T. (2006). Fiber to the home/fiber to the premises: What, where, and when. *Proceedings of the IEEE*, 94(5), 911–934.
6. Qiu, X.-Z., Ossieur, P., Bauwelinck, J., Yi, Y., Verhulst, D., Vandewege, J., et al. (2004). Development of GPON upstream physical-media-dependent prototypes. *IEEE Journal of Lightwave Technology*, 22(11), 2498–2508.
7. Oh, Y.-H., Lee, S.-G., Le, Q., Kang, H.-Y., & Yoo, T.-W. (2005). A CMOS burst-mode optical transmitter for 1.25-Gb/s ethernet PON applications. *IEEE Transactions on Circuits and Systems II: Express Briefs*, 52(11), 780–783.
8. Agrawal, G. P. (2002). *Fiber-optic communication systems* (3rd ed.). New York, NJ: John Wiley & Sons.
9. Gigabit-capable Passive Optical Networks (GPON). (2003). Physical media dependent (PMD) layer specification, ITU-T Recommendation G.984.2.
10. Faucher, J., Mukadam, M. Y., Li, A., & Plant, D. V. (2006). 622/1244 Mb/s burst-mode CDR for GPONs. In *Proceedings of IEEE Laser and Electro-Optics Society (LEOS) Annual Meeting*, Montreal, QC, Canada, October, Paper TuDD3.
11. Shastri, B. J., Faucher, J., Zeng, M., & Plant, D. V. (2007). Burst-mode clock and data recovery with FEC and Fast phase acquisition for burst-error correction in GPONs. In *Proceedings of IEEE Midwest Symposium on Circuits and Systems (MWSCAS)*, Montreal, QC, Canada, August, pp. 120–123.
12. Eldering, C. A. (1993). Theoretical determination of sensitivity penalty for burst mode fiber optic receivers. *IEEE Journal of Lightwave Technology*, 11(12), 2145–2149.
13. Ossieur, P., Qiu, X.-Z., Bauwelinck, J., & Vandewege, J. (2003). Sensitivity penalty calculation for burst-mode receivers using avalanche photodiodes. *IEEE Journal of Lightwave Technology*, 21(11), 2565–2575.
14. Goodman, J. W. (2000). *Statistical optics*. New York, NJ: Wiley.
15. Sklar, B. (2001). *Digital communications: fundamentals and applications* (2nd ed.). Upper Saddle River, NJ: Prentice-Hall.
16. Kartalopoulos, S. V. (2004). *Optical bit error rate: an estimation methodology*. New York, NJ: Wiley.
17. Ogawa, K. (1982). Analysis of mode partition noise in laser transmission systems. *IEEE Journal of Quantum Electronics*, 18(5), 849–855.
18. Agrawal, G. P., Anthony, P. J., & Shen, T. M. (1988). Dispersion penalty for 1.3- $\mu$ m lightwave systems with multimode semiconductor lasers. *IEEE Journal of Lightwave Technology*, 6(5), 620–625.
19. Liu, X., Lu, C., & Cheng, T. H. (2005). Forward error control in passive optical networks. In *Proceedings of Optical Fiber Communication (OFC) Conference*, Vol. 1, Anaheim, CA, March, p 3.
20. Yi, Y., Verschuere, S., Lou, Z., Ossieur, P., Bauwelinck, J., Qiu, X.-Z., et al. (2008). Simulations and experiments on the effective optical gain of FEC in a GPON uplink. *IEEE Photonics Technology Letters*, 19(2), 82–84.
21. Jagath-Kumara, K. D. R., & Bebbington, M. (2005). Error content in frames transmitted over burst-error channels. *IEEE Transactions Wireless Communications*, 4(5), 2533–2539.
22. Hagelbarger, D. W. (1959). Recurrent codes: easily mechanized, burst-correcting, binary codes. *Bell Systems Technical Journal*, 38, 969–984.

the top 5%. He is a reviewer for the Computer Vision and Image Understanding (CVIU) Journal and Machine Vision and Applications (MVA) Journal, a student member of IEEE-LEOS and the Optical Society of America (OSA), and the current Vice-President of the McGill OSA Student Chapter.



Julien Faucher received the Ph.D. degree in Electrical Engineering from McGill University, Montreal, Canada, in 2006. He has been working at PMC-Sierra, in the mixed-signal group, since 2005. His research interests include burst-mode receivers, clock and data recovery circuits, and mixed-signal design and verification. Dr. Faucher received graduate scholarships from the Natural Sciences and Engineering Research Council of Canada (NSERC) and from Le Fonds

pour la Formation de Chercheurs et l'Aide à la Recherche du Québec (FCAR). He was also awarded a Richard H. Tomlinson Doctoral Fellowship from McGill University.



Noha Kheder was born in Cairo, Egypt. She received the B. Eng. degree (with distinction) in Electrical Engineering from McGill University, Montreal, QC, Canada, in 2006, where she is currently working toward the M.Eng. degree in Electrical Engineering. Her research interests include passive optical networks and burst-mode receivers for passive optical networks. Ms. Kheder is the recipient of a Master's research scholarship from Le Fonds Que-

becois de la Recherche sur la Nature et les Technologies (FQRNT). She